GLIA 51:121–131 (2005)

Activity-Dependent Change in Morphology of the Glial Tubular Lattice of the Crayfish Medial Giant Nerve Fiber

JOSEPH E. BESHAY,[†] PAULETTE HAHN,[†] VICTOR E. BESHAY,[†] PAL T. HARGITTAI, AND EDWARD M. LIEBERMAN[1]*
Department of Physiology, Brody School of Medicine at East Carolina University, Greenville, NC 27834

KEY WORDS
axon; glia; tubular lattice; electron microscopy; potassium; TEA

ABSTRACT
An evaluation of electron micrographs of stimulated nerve fibers used to investigate the effect of action potential generation on the structure–function relationship between axons and its associated glial cells revealed that what was at first thought to be stimulation-induced damage to the glia was, in fact, limited to volume expansion and disaggregation of the glial tubular lattice. All other structures appeared well preserved and otherwise normal. Using a 4-point subjective scale for evaluation by two investigators, 50-Hz stimulation for 2 min was observed to cause a volume expansion and disaggregation of the tubular lattice. Quantitatively, the internal diameter of the stimulated tubular lattice increased 65% above the unstimulated control (50.96 ± 2.09 nm and 30.81 ± 0.87 nm, respectively, $P \leq 0.001$). Stimulation had its greatest effect on tubular lattice volume and organization in the adaxonal glial layer and a decreasing effect as distance from the giant axon increased. These effects are reversible since the tubular lattice diameter and degree of disaggregation preserved 10 min after the cessation of stimulation were not found to be different from their unstimulated paired controls. Axons injected with TEA, a voltage-gated potassium channel blocker, prevented stimulation-induced volume expansion and disaggregation of tubular lattice structure. These results are consistent with an active uptake of K^+ with obligated water or, alternatively, hyperosmotic K^+ uptake and a fixation-induced increase in water permeation. Either mechanism of K^+ uptake would result in tubular lattice volume expansion and disaggregation and suggests that the tubular lattice serves a larger role than a simple transglial diffusion pathway.

INTRODUCTION

The role of the periaxonal glial cell layer in regulating the K^+ released by nerve axons during repetitive action potential generation has been the subject of investigations for decades. In their studies of the squid giant axon, Frankenhauser and Hodgkin (1956) suggested that the associated Schwann cell layer represented a passive barrier that restricted diffusion of K^+ from the adaxonal space with a time constant for its clearance of 50–100 ms. A decade later, Orkand et al. (1966) provided evidence, using an amphibian optic nerve preparation, that small quantities of extracellular K^+ could be rapidly cleared from the periaxonal space by a spatial buffering mechanism. Spatial buffering depends on axonally released K^+ inducing a depolarization of the adaxonal surface of glial cells and K^+ inward rectifier channels that rapidly transports ion from the adaxonal surface through the cell to be released to more lateral extracellular spaces. Reinvestigations of K^+ clearance from both squid and crayfish giant nerve fibers (Shrager et al., 1983; Pichon et al., 1987; Abbott et al., 1988) have shown that K^+ clearance is, in fact, quite rapid (10 ms) in carefully prepared and well-oxygenated nerve fiber preparations. Based on mathematical models of the extracellular space that included the glial tubular lattice as proposed by Brown and Abbott (1993), Inoue et al. (1997) used pulsed voltage-clamp to evaluate K^+ current inactivation kinetics and K^+ accumulation resulting from propagated action potentials. Their results led them to argue that diffusion alone can account for rapid clearance of K^+ from the adaxonal space of the squid giant axon.

In earlier studies of K^+ accumulation and clearance in crayfish medial giant nerve fibers (Brunder and Lieberman, 1988; Hassan and Lieberman, 1988; Lieberman and Hassan, 1988), it was evident that much of the stimulation-induced release of K^+ from axons was taken up by the associated glia in a quantity that resulted in glial cell swelling when conditions favored accumulation of extracellular K^+ in the adaxonal space. When conditions did not favor extracellular K^+ accumulation (e.g., low resting membrane conductance or low external K^+ concentration) there was a slight decrease or no change in glial volume. The K^+ accumulated by glia was presumably released back to the extracellular space for uptake by the axon, as suggested by the return of glial cell volume and the stimulation-induced glial membrane hyperpolarization to normal values during several minutes after the cessation of stimulation. These findings lead to the hypothesis that the physiologically induced glial hyperpolarization, which reduced the outwardly directed electrochemical gradient for glial K^+, participates in the process of ionic homeostasis of the

*Correspondence to: Edward M. Lieberman, Department of Physiology, Brody School of Medicine, East Carolina University, Greenville, NC 27834.
E-mail: liebermane@mail.ecu.edu

[†]These individuals contributed equally to this investigation and are to be considered as co-first authors.

Received 5 July 2004; Accepted 7 January 2005

DOI 10.1002/glia.20192

Published online 23 March 2205 in Wiley InterScience (www.interscience.wiley.com).

perineural space (Hassan and Lieberman, 1988; Lieberman and Sanzenbacher, 1992).

Concurrent with these physiological studies, ultrastructural studies of squid and crayfish adaxonal glial cells (Hama, 1962; Paracchia and Robertson, 1971; Shivers and Brightman, 1976; Lieberman et al., 1981), Zwahlen et al. (1988) identified and described a network of tubules, now referred to as the tubular lattice. The tubular lattice appears to be derived from invaginations of the glial cell membrane with openings to both adaxonal and lateral extracellular space regions. It has been proposed that the tubular lattice could serve as a mechanism for shorter and multiple parallel diffusion pathways across the glial layer than that provided by the mesaxonal cleft pathways around glial cells (Shrager et al., 1983, Brown and Abbott, 1993). Evidence provided by Holtzman et al. (1970) and Lane et al. (1977) that deposition of horseradish peroxidase (HPO) and La^{3+} occurs in the tubular lattice is consistent with the hypothesis that the lattice is open to diffusion.

Although a number of investigators have hypothesized that the tubular lattice can serve to clear K^+ from the adaxonal space in a manner consistent with diffusion across the glial layer, no experimental evidence has been provided for such a mechanism. The purpose of the present investigation was to combine ultrastructural with physiological studies to shed light on the function of the glial tubular lattice in crayfish medial giant nerve fibers.

MATERIALS AND METHODS

Materials

Gluteraldehyde, osmium tetroxide (OsO_4), Epon 812 resin, propylene oxide, uranyl acetate, maleic acid, Kodak 4489 electron microscopy film, and Kodak Polycontrast III RC photographic paper were obtained from Electron Microscopy Sciences, Ft. Washington, PA. Ethanol, veronal acetate (barbitol), tetraethylammonium salt (TEA), and salts for physiological solutions were obtained from Fisher Scientific.

Animals and Tissue Preparation

Crayfish, *Procambarus clarkii*, ranging in length from 4 to 6 inches, were obtained commercially from Wauban Laboratories, Schreiver LA and Atchafalya Biological Supply (Raceland, LA). The ventral nerve cord was removed from the animal and placed in a plexiglas chamber and continuously superfused with a normal physiologic crayfish solution (NCS). NCS contains (in mM), 190 NaCl, 5.4 KCl, 13.5 $CaCl_2$, 2.6 $MgCl_2$, and 20 Tris-HCl, at pH 7.4. The sheath surrounding the nerve cord (the blood-brain barrier) was removed to allow individual giant nerve fibers to be more easily visualized as well as to reduce diffusion restrictions to the axons and associated glia, thereby ensuring rapid access of morphological tracers ($LaCl_3$), pharmacological agents, and fixatives for electron microscopy to the axon and associated glial layer. All experiments were performed at ambient room temperature (21–23°C).

Electrophysiology

Giant nerve fibers were impaled with glass microelectrodes for monitoring of resting and action potentials for a period of ~30 min following its isolation from the animal to ensure that the nerve fibers were not damaged by nerve cord isolation and desheathing procedures. Only axons that were capable of propagating action potentials through the thoracic nerve cord for 2 min at 50 Hz were used in the experiments.

Depending on the experimental protocol, one or both sides of the nerve cord were stimulated with external electrodes in contact with the circumesophageal connectives to generate propagated action potentials. For paired control experiments, one circumesophageal connective was severed at the cephalic ganglion. The severed connective was moved away from the external stimulation electrodes to prevent its stimulation. The severed side was examined electrophysiologically to ensure that it did not generate APs when the intact side was stimulated.

Just before the beginning of each experiment, a physiological saline containing veronal acetate as a buffer was substituted for Tris-buffered NCS. Veronal acetate had no short-term effects on the electrical or morphological properties of the tissue but improved preservation of the tissue as compared to normal Tris-buffered solutions. At the end of the 2-min stimulation period the nerve cord was superfused with 2% gluteraldehyde in NCS with 40 mM veronal acetate, pH 7.4. Stimulation continued during fixation until action potentials could not be elicited (1–3 min). When membrane potential of the axon fell to approximately −50 mV (~20 min) the tissue was removed from the recording chamber after dividing the cord into right and left hemiconnectives. These tissue segments were placed in vials containing 2% gluteraldehyde and stored at 4°C overnight before further preparation for electron microscopy.

For $LaCl_3$ precipitation, the tissue was superfused with 5 mM $LaCl_3$ in NCS followed by superfusion with 2% glutaraldehyde in a solution containing in mM; 100 Na_2SO_4, 5.4 KCl, 1.0 $CaCl_2$, 2.7 $MgCl_2$, 40 vernal acetate at pH 7.4, and 430 mOs.

Oil-filled glass micropipette cannulae, originally described by Wallin (1967) for sampling of axoplasm from crayfish medial giant axons, were used for the experiments in which TEA was injected into the medial giant axon.

Electron Microscopy Processing

After appropriate washing, postfixation was achieved with 1% osmium tetroxide (OsO_4) in veronal acetate buffered NCS for 1 h at 4°C. En bloc staining was accomplished with 1% uranyl acetate in 0.05 M maleic acid (pH 5.2) for 1 h. The tissue was then dehydrated in an increasing series of ethanols, followed by propylene oxide. Subsequently, the tissue was infiltrated and embedded with Epon 812 resin. The blocks were then polymerized at 65°C for 48 h. Following this, blocks were trimmed and thinly sectioned using a diamond knife. Grids were

prepared and restained with 2% uranyl acetate and lead stained in a traditional fashion. Grids were viewed using a JOEL transmission electron microscope, and micrographs were obtained on Kodak 4489 electron microscopy film. Prints from negatives or the negatives themselves were digitized and used to make the final figures.

Morphometrics

Stereological methods for quantification of ultrastructural characteristics of the crayfish medial giant nerve fiber were used as described in Weibel (1979). Data in the form of the number of intersections of a reference grid system with structures seen in electron micrographs were collected. Estimates of volume, surface area length, and relative number of organelles determined mathematically and statistically could be determined. The crayfish thoracic nerve cord was cut into interganglionic segments. Two grids of ultrathin cross sections were collected from each of three interganglionic segments for each animal, i.e., a total of six samples per animal. The field selected for morphometric analysis was photographed at a primary magnification of 10,000× and a photographic print enlargement totaling 25,000×. The grid used for the analysis was a 10 × 10-cm transparent plate divided into 10.05 × 10.05-mm squares.

For evaluation of structure-function relationships of the giant axon and its surrounding glial cell layers, as related to K^+ homeostasis, the periaxonal region of the medial giant nerve fiber was located and photographed at an initial magnification of 15,000×. Two methods were used to assess the "quality of preservation" of the tubular lattice of unstimulated and stimulated nerve fibers. For clarity, "quality of preservation" is defined as the assessment of the cross-sectional area (volume) of the tubules of the tubular lattice and its degree of aggregation (structural organization).

The first method involved the qualitative evaluation of electron micrographs from each experiment by two independent investigators, one of whom was blinded to the experimental protocol. The investigator examined and assigned a subjective score to each experiment and its control using a 4-point scale (1–4), where 4 represented a high degree of aggregation and compactness (small cross-sectional area) of tubular lattice structures. The second method was quantitative and used computerized measurements of the inner diameter of the opening of a tubule of the tubular lattice. Electron micrographs were digitized and displayed on a computer monitor at high magnification. The number of pixels across the diameter of a tubular lattice opening was recorded and entered into an Excel spreadsheet. Only openings that had a near circular form were used for these measurements. The inner diameter of the tubular lattice was converted to nm by the equation:

$$\text{TL diameter (nm)} = (\text{TL diameter in pixels})/(\text{pixels/cm}) \times (\mu\text{m/cm}) \times 1000$$

Statistical analysis was carried out by GraphPad Instat using a paired or unpaired (two-tailed) *t*-test, as justified by the experimental protocol. Numerical values were given as population mean ±1 SEM. Differences between population means were considered significant at $P \leq 0.05$.

RESULTS

Normal Morphology

A collage of four electron micrographs (Fig. 1) illustrates the cross-sectional structure of the hemiconnective from the axolemma and cortical axoplasm of the medial giant axon (upper left) to the dorsal surface of the connective (lower right). It includes the medial giant axon, adaxonal and more lateral periaxonal glial layer, an outer layer of small nerve fibers with their associated glia, blood-brain barrier, and perineurial sheath that faces the body fluid compartment. Large numbers of tubular lattice clusters are seen in the adaxonal and periaxonal glial layers. By visual examination, the cross-sectional area of tubules seen face-on or the diameter of the tubules seen in longitudinal section were not different between adaxonal and periaxonal glial layers.

The medial giant axon is surrounded by concentric layers of glia separated by layers of collagen. The adaxonal glial layer is composed of multiple glial cells interdigitated to form a compact barrier that separates the axon from the more lateral and loosely organized glial cells and collagen layers. The extensive and highly organized tubular lattice is shown in higher magnification in Figure 2A. More than one tubular lattice cluster may be found in individual glial cells. As indicated by the arrows, the adaxonal glial layer opens to the axonal-glial space and the glia–collagen interface as well as glia–glial interfaces (Fig. 2B,C). In the outer layers of glia, the tubular lattice opens to glia–collagen interfaces on both sides of the glial cell. Although the tubular lattice is found throughout all layers of the nerve cord its frequency of appearance decreases with distance from the giant axon. No tubular lattice is seen in the perineurial sheath lateral to the blood-brain barrier.

Stereology

Measurements of the various parameters of relevant structures of the interganglionic connective are tabulated in Table 1. Glial cells form 40 ± 2% of the total barrier volume associated with the medial giant axon and the adaxonal layer accounting for 25% of the total glial cytoplasm. Collagen makes up only 2% of the adaxonal layer volume. Visual examination of the adaxonal glia suggests that they are more tightly interdigitated than the glia in the outer layers. This is confirmed by measurement. Glial–glial interface surface density is approximately 2 times greater in the adaxonal layer than in outer glial layers (6.47 ± 0.58 and 3.77 ± 0.33, respectively). Further evaluation of the glial membrane facing the axon compared to that facing the collagen space gave a 5 times greater surface density for the glia–collagen interface.

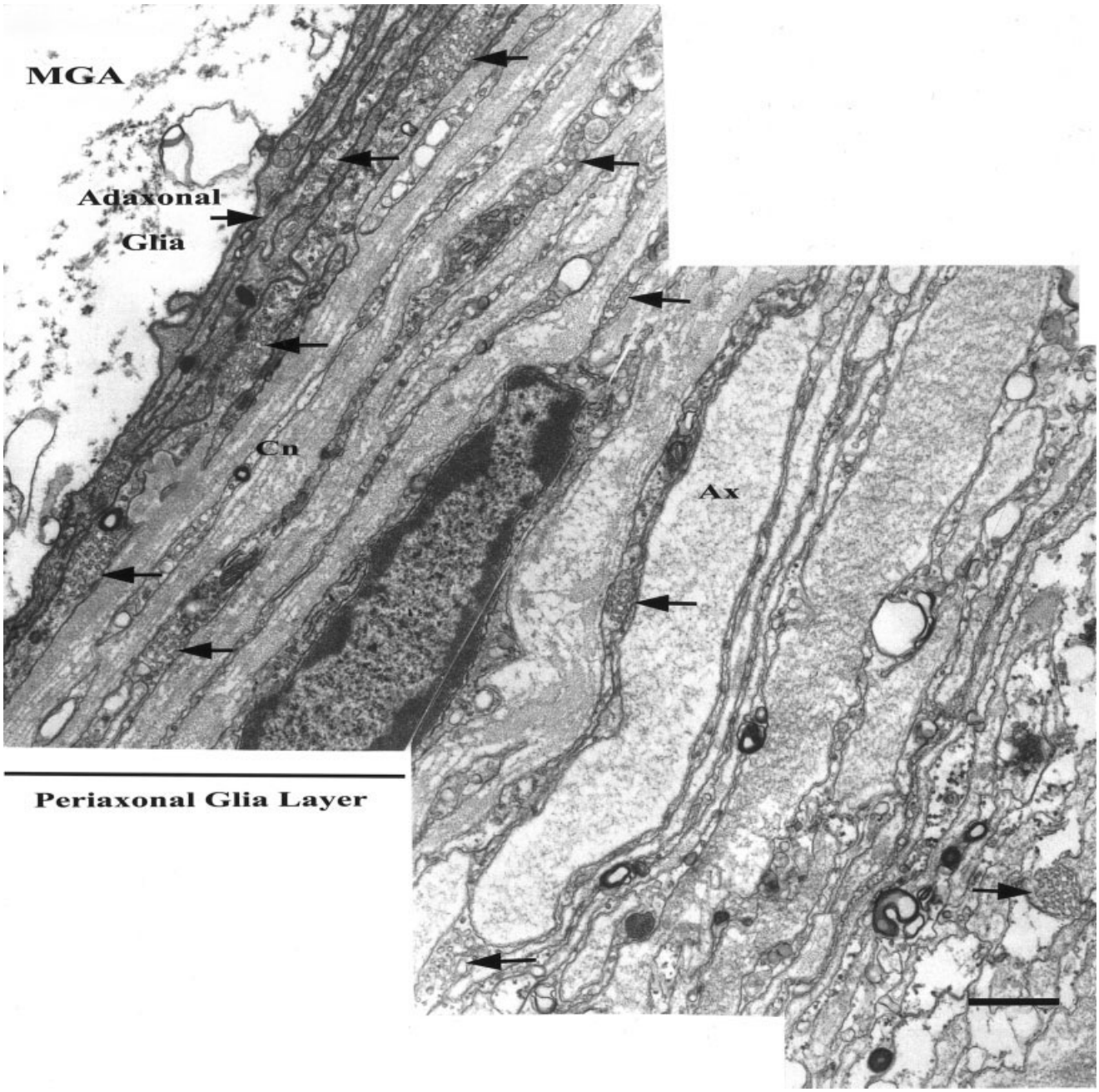

Fig. 1. Normal structure of a hemiconnective of the crayfish ventral nerve cord. This electron micrograph is a collage of four photographs representing a cross section through a hemiconnective spanning the distance from the cortical region of the axoplasm of the medial giant axon (MGA), through the associated adaxonal glial layer (Ad), periaxonal glial layer with its multiple layers of collagen (Cn), small axons (Ax), perineurial glia serving as the blood-brain barrier (BBB), and neural lamella. Together, the perineurial glial layer and lamella serve as the perineurial sheath. The arrows indicate the positions of glial tubular lattice clusters. The numbers of clusters are greatest in the adaxonal glial layer with a decreasing appearance in the perineural glial layer. Tubular lattice clusters are found associated with small axons, but not at the same frequency seen with the medial giant axon. Clusters of tubular lattice are also seen in glial cytoplasm in the periaxonal glial layer associated with collagen. There are no tubular lattice clusters beyond the perineurial glial layer. Scale bar = 5 μm.

Consistent with the high metabolic activity of the adaxonal glial layer and its postulated role in ion transport and adaxonal space homeostasis (Hargittai and Lieberman, 1991; Lieberman et al., 1994) mitochondria, as a volume fraction (percentage of total glial cytoplasmic volume), was 3.8 ± 0.5% and approximately 2 times that found in the outer glial layers.

The tubular lattice was approximately 5 times more prevalent in the adaxonal glial layer than in the outer layers. In the adaxonal layer, for each opening to the adaxonal space, the tubular lattice opened to the adjacent glia 4 times and to the adjacent collagen layer, 3 times. Overall there were approximately eight openings to any surface for each patch of tubular lattice. When the volume of the tubular

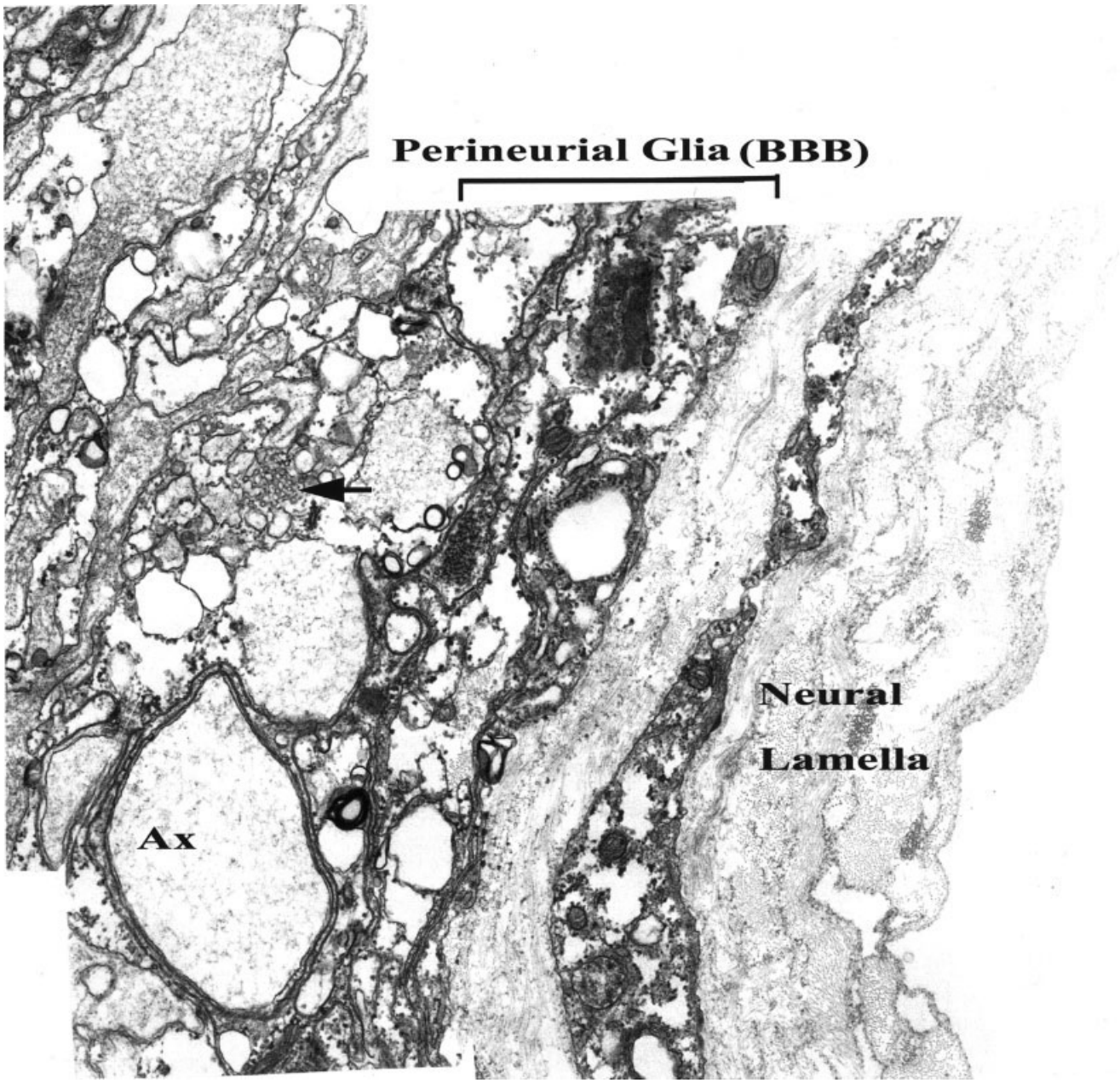

Figure 1. (Continued)

lattice is normalized to 1 μm^3 of glial cytoplasm there were 30 tubular lattice openings to any surface in the adaxonal glia and 15 in the outer layer. The mean length of the distance across the adaxonal glial barrier via the space between glia (mesaxon) averages 4.32 μm. Assuming that the tubular lattice opens to the adaxonal, glia–glial, and glia–collagen spaces and permits free diffusion of substances into and through the tubules, the mean diffusion length across the glia is reduced to 0.38 μm when the multiple parallel pathways of the tubular lattice are included. This represents a reduction in the diffusion path by an order of magnitude (Table 1). The average internal diameter of the tubules, as seen face on, is ~31 nm (Fig 3, top).

Distribution of La^{3+} in the Inner Glial Layer

Following incubation of the intact desheathed nerve cord with 5 mM $LaCl_3$ and its precipitation with a Na_2SO_4 containing fixative solution, there was an appearance of precipitated Lanthanum in the glial intercellular spaces, within the tubular lattice and in the adaxonal space. This result is consistent with earlier investigations of the tubular lattice by Lane et al. (1977). The intensity of La^{3+} deposition increased with the time of incubation and stimulation (Figs. 2C and 4). In nerve fibers examined without $LaCl_3$ precipitation there was no evidence of high-affinity La^{3+} binding sites. During the incubation and before

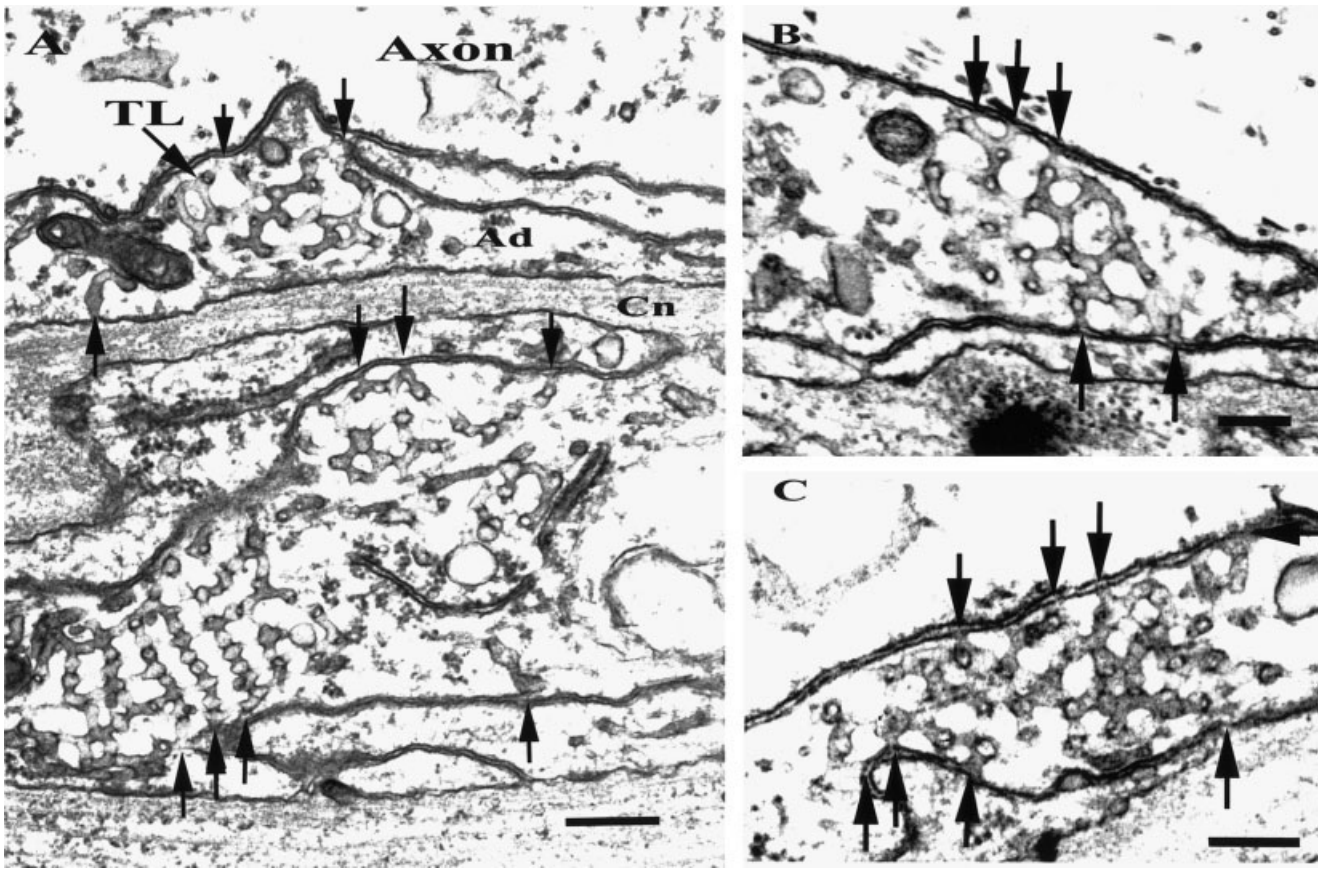

Fig. 2. Glial tubular lattice structure and its associations with adjacent glia, collagen, and medial giant axon. **A:** Morphology of the tubular lattice cluster. Note numerous openings of the tubular lattice to both the glial/axon, glial/glial, and glial/collagen interfaces (arrows). The organized structure of the tubular lattice appears in several forms depending on the orientation of the section. Note "string-of-beads" organization of the tubular lattice in the lower left tubular lattice cluster and the different but regular patterns in B and C. It is clear from A and from B and C that the tubular lattice effectively short circuits the tortuous mesaxonal (glial/glial) pathway from the axolemma to the collagen layer with multiple parallel pathways that could serve as diffusion pathways to or from the axolemma. **B:** High-magnification electron micrographs of an adaxonal tubular lattice cluster. Arrows indicate the openings of the tubular lattice to the glial/axonal and glial/glial interfaces. **C:** Tubular lattice also shows a similar relationship to the glial/axonal, glial/glial, and glial/collagen interfaces with numerous openings of the tubular lattice to the various spaces. In addition, this nerve fiber was incubated with 5 mM $LaCl_3$ for 15 min and precipitated with Na_2SO_4 simultaneously with the fixation protocol. The La^{3+} precipitate can be seen along the glial/axonal interface and an increased density in the lumen of the tubular lattice indicating that it is open to the extracellular space for entry by small ionic substances. Scale bars = 0.2 μm in A; 0.1 μm in B,C.

precipitation resting and action potentials were monitored. Action potential duration, which ranges from 0.5 to 0.8 ms in untreated preparations, increased to 1.0–2.4 ms within 5 min, indicating that La^{3+} reached the axon membrane more rapidly than can be detected morphologically.

Stimulation with electrical pulses of 0.5 ms duration at 50 Hz/2 min, to generate propagated action potentials in the presence of $LaCl_3$, led to an increase in the appearance of precipitated La^{3+} in the tubular lattice and heavy staining of glia–axonal and glia–glial spaces. Deposition of La^{3+} by high-frequency propagated action potential generation was accompanied by a swelling and an apparent disaggregation of the tubular lattice (Fig. 4). It is also notable that the number of openings of the tubular lattice to the interglial and adaxonal space appear to be dramatically reduced with stimulation (Figs. 4 and 5A) as compared with the tubular lattice of nonstimulated nerve fibers (Fig. 2).

Depolarization of the giant axon (10 mV/100 ms at 2 Hz for 30 s) by application of square pulse currents with an intracellular axial wire caused a dense filling of the tubular lattice with La^{3+} along with a disruption of both glial and axonal membranes and vacuolization of the glial cytoplasm (not shown). Even in these extreme conditions glial mitochondria and nuclei appeared to be relatively intact.

For all experiments involving nerve excitation, external stimulation of the circumesophageal connective was used to produce propagated action potentials. Effects of stimulation and treatments were monitored in a distant thoracic interganglionic connective to avoid the degree of morphological disruption of the adaxonal glial layer seen with axial wire stimulation.

Effect of Stimulation on Morphology of Glia Associated With Medial Giant Axon

It is not clear from the above experiments whether stimulation of the nerve tissue or its exposure to $LaCl_3$ was the cause of the swelling and disaggregation of the

TABLE 1. Morphometry of the Crayfish Medial Giant Nerve Fiber

Structure	Measurement[a]	Range
Axon diameter[b] (μm)	169 ± 4; n=130	91–315
Glial cell volume fraction (%)	40 ± 2	
Collagen matrix volume fraction (%)	56 ± 2	
Intercellular space volume fraction (%)	4 ± 0.3	
Mean barrier thickness (μm)		
Adaxonal glial layer	0.29 ± 0.02	
Outer glial layer	2.44 ± 0.21	
Total	3.18 ± 0.28	
Mean no. of glial layers	11	6–16
Axon:Schwann cell membrane ratio[c]	1:11	
Total glial cells/cross section[d]	19	12–28
Tubular lattice		
Adaxonal volume fraction (%)	6.7 ± 1.2	
Outer layer volume fraction (%)	1.2 ± 0.5	
Mean tubular inner diameter (nm)	30.81 ± 0.87	20–60
Mean openings per patch	8	
Glia–glia interface length[e]		
Without tubular lattice (μm)	4.32	
With tubular lattice (μm)	3.79	

[a]Values are given as mean ± 1 SEM.
[b]Randomly selected from axons used for experiments in this laboratory (1985–1989).
[c]Hargittai and Lieberman (1991).
[d]Lieberman et al. (1981).
[e]These values are estimated from the average three-dimensional pathway per unit volume of glia by calculating the length density (14.9 ± 2.5 μm^{-2} and 13.1 ± 2.2 μm^{-2}, respectively) and average barrier thickness.

TABLE 2. Effect of Stimulation and TEA on Quality of Preservation of Tubular Lattice in Adaxonal Glia of the Crayfish Medial Giant Nerve Fiber

Preservation	Nonstimulated[a]	Stimulated	*P*
No drug	3.22 ± 0.20 (15)	2.33 ± 0.13 (15)	≤0.001[b]
TEA	3.00 ± 0.08 (4)[d]	3.38 ± 0.26 (4)[c]	≤0.05[c]; ≤0.09[d]

[a]All values given as mean ± 1 SEM (n = number of individual axons examined).
[b]Stimulation vs. nonstimulation for paired comparisons.
[c]Stimulation with TEA vs. stimulation without TEA (unpaired).
[d]Nonstimulation with TEA vs stimulation with TEA.

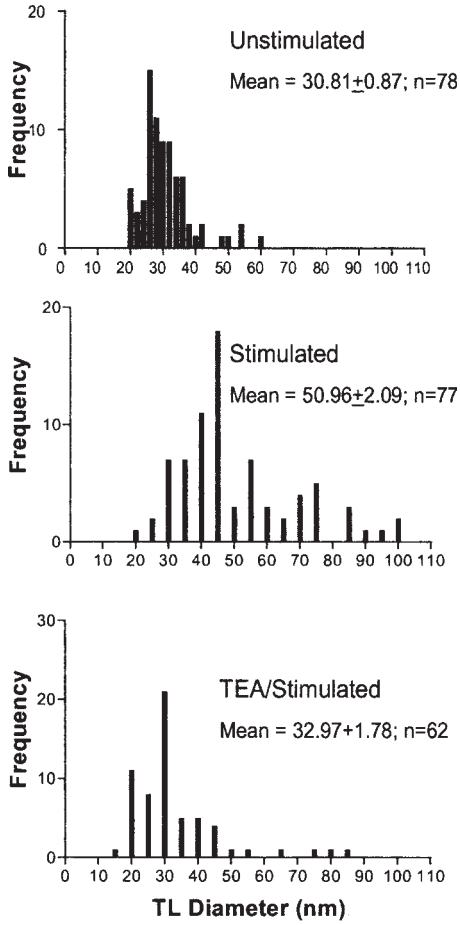

Fig. 3. Effects of stimulation and TEA on the internal diameter of the tubular lattice. *Top*: Tubular lattice diameters in glia of resting untreated unstimulated nerve fibers show a tight distribution of internal diameters around 30 nm. *Middle*: Stimulation at 50 Hz/2 min cause a major increase in tubular lattice diameter (51 nm) with a much larger internal diameter distribution range. *Bottom*: Following injection of TEA in to the axon and stimulation at 50 Hz for 2-min diameters of the tubular lattice are not statistically different from controls. The diameter distribution range is similar to the control although a few larger diameters are seen. Values for tubular lattice diameter given with each panel are means ± 1 SEM; n = the number of tubules measured from 12 electron photomicrographs of three nerve cords (top two panels) and 10 electron photomicrographs from four nerve cords (bottom).

tubular lattice in the glial layer. Examination of tissue stimulated in the absence of $LaCl_3$ demonstrated clearly that stimulation was the major, if not the sole factor in the morphological changes of the tubular lattice preserved by fixation, i.e., volume expansion and disaggregation (Table 2, Fig. 3, middle). Of significance, there was little change in nuclei or mitochondria (Fig. 5A). Tubular lattice of glial layers more distant from the axons indicated they were less affected by stimulation. This finding is illustrated in Figure 5B and demonstrates the tubular lattice furthest from the giant axon is not distinguishable from the unstimulated controls.

To control further for the effects of stimulation on the tubular lattice the tissue was stimulated at 50 Hz for 2 min with fixation delayed for 10 min. In this case, the tubular lattice of control unstimulated nerve and nerve stimulated but rested for 10 min before fixation and preparation for electron microscopy could not be distinguished from each other with regard to the appearance of the tubular lattice (data not shown). This result was not be unexpected considering that the crayfish nerve fiber can be stimulated at high frequency for tens of minutes, even to exhaustion, and be stimulated again after a short period of rest with no apparent physiological damage (Hassan and Lieberman, 1988).

Effect of K^+ Channel Blockade by TEA on Stimulation-Induced Tubular Lattice Morphological Changes

A primary function of glial cells in association with the medial giant axon of the crayfish is regulation of the ionic content of the adaxonal space. During action potential generation, significant efflux of K^+ occurs and, unless rapidly cleared from the adaxonal space, the signaling properties of the axon may be compromised. The following experiments were predicated on the hypothesis that the tubular lattice is directly involved in K^+ uptake, sequestration and compartmentalization of K^+ released during action potential generation resulting in tubular lattice volume expansion and apparent disaggregation. Limiting K^+ efflux from the axon from the axon during excitation should prevent or lessen the morphological change in the tubular lattice.

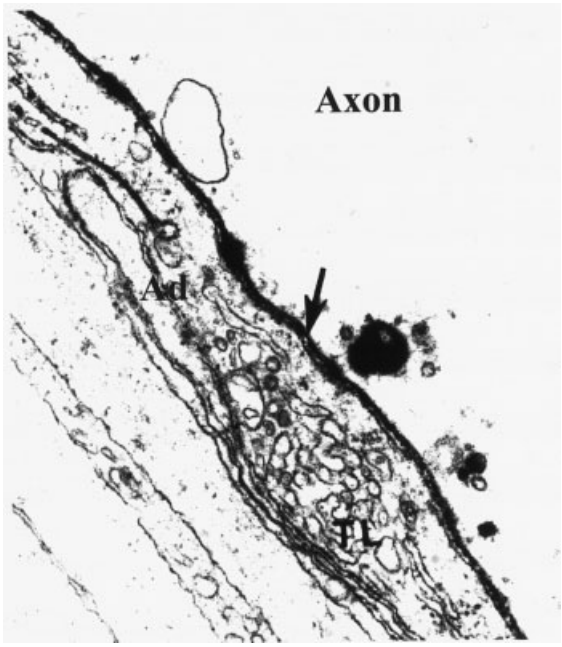

Fig. 4. Effect of the duration of incubation and stimulation on La^{3+} precipitation in glial/axonal and glial/glial interfaces and in the tubular lattice. La^{3+} precipitate seen in the glial/axonal, glial/glial interface, as well as in the tubular lattice, is dramatically increased, as compared with that seen in Fig. 2C, when the time of incubation with $LaCl_3$ is increased to 30 min. With stimulation (50 Hz, 1 min) the tubular lattice appears swollen and structurally disorganized. Scale bar = 0.1 μm.

A 4–8-nl bolus of 0.5–1 M tetraethylammonium (TEA), a membrane impermeant voltage-gated K^+ channel blocker, was injected into the axon at the most caudal double ganglion and allowed to diffuse into more cephalic portions of the axon (~30–45 min). During this period, resting and action potentials (0.5–1-Hz stimulation) of the medial giant nerve fiber were monitored in the hemiconnective that was to be used for morphological analysis.

When action potentials in this region become elongated (2–4-ms duration), indicating that the voltage-gated K^+ channels had been blocked by TEA, the nerve fiber was stimulated at 50 Hz/2 min and was fixed for electron microscopic analysis. The results of these experiments are tabulated in Table 2 and Figure 3 (bottom).

By visual examination, the appearance of glial tubular lattice clusters in stimulated TEA-injected nerve fibers could not be distinguished from those injected with TEA but not stimulated, nor were the former distinguishable from the untreated nonstimulated control nerve fibers. Quantitative measurements of the cross-sectional diameter of the glial tubular lattice of TEA injected and stimulated nerve fibers demonstrated that the average diameter was not statistically different from the control. These results suggest that limiting K^+ efflux from excited axons reduced tubular lattice swelling and disaggregation, as seen in untreated stimulated nerve fibers.

DISCUSSION

Preliminary studies from our laboratory during the late 1980s that attempted to preserve electrically stimulated crayfish medial giant nerve fibers for electron microscopic examination was abandoned because of our perception that the tissue appeared damaged by stimulation. A reexamination of these electron micrographs, with the investigations by Wurtz and Ellisman (1986, 1989) of reversible transient activity-induced swelling of the Schwann cell folds of the vertebrate node of Ranvier in mind, revealed that the morphological changes induced by stimulation of the crayfish medial giant nerve fiber was limited to the tubular lattice system of the adaxonal glia, leaving membranes, mitochondria, and nuclei unchanged. This study focused on a reexamination of the concept that the tubular lattice serves only as a simple ion diffusion pathway with the goal to provide experimental evidence for a structural basis for K^+ clearance from the adaxonal space of axons stimulated at high frequency.

Inoue et al. (1997) using a pulsed voltage clamp protocol and K^+ current inactivation analysis suggests that K^+ clearance from the adaxonal space can be accounted for by passive diffusion through the inter-glial spaces and glial tubular lattice structures in the squid giant nerve fiber. There are two lines of evidence that make it unlikely that diffusion, alone, can account for K^+ clearance from the crayfish medial giant nerve fiber. The first is seen in a comparison of the resistance in series with the axon membrane (R_s) of the squid giant nerve fiber with that of the crayfish. R_s represents the electrical resistance of the pathway for ionic movement through and around the glial barrier that separates the axolemma from the bulk extracellular space. Using a construct developed by Adelman et al. (1977), Brown and Abbott (1993) developed a mathematical model of the diffusion pathways through the squid glial layer. They calculated an R_s for the inter-glial pathway of ~20 Ωcm^2. Including the tubular lattice in the model reduced the calculated R_s to ~2 Ωcm^2, a value consistent with the electrically measured R_s of the squid glial layer. In contrast the R_s of the crayfish glial layer is 9–12 Ωcm^2 (Hassan and Lieberman 1988). For a passive diffusion model, the time constant for K^+ clearance from the adaxonal space of the squid nerve fiber should be up to 5-fold faster than that measured in the crayfish. In fact, the opposite has been measured (Shrager et al., 1983; Pichon et al., 1987). It appears that crayfish utilize highly effective mechanisms, e.g., K^+ uptake by the tubular lattice, to overcome the potential for excessive K^+ accumulation that might occur with a high R_s and diffusion as the primary or sole clearance mechanism.

The second line of evidence is found in the effect of glial membrane transporters and glial receptor agonists and antagonists on K^+ uptake from the adaxonal space of crayfish and squid. In the crayfish, ACh and d-TC acting on the glial cholinergic receptor, shown to alter glial membrane potential and K^+-induced glial volume regulation, a Na^+-pump inhibitor (ouabain) and a Na^+, K^+, $2Cl^-$ cotransporter inhibitor (bumetanide), altered glial volume significantly in the presence of high-frequency stimula-

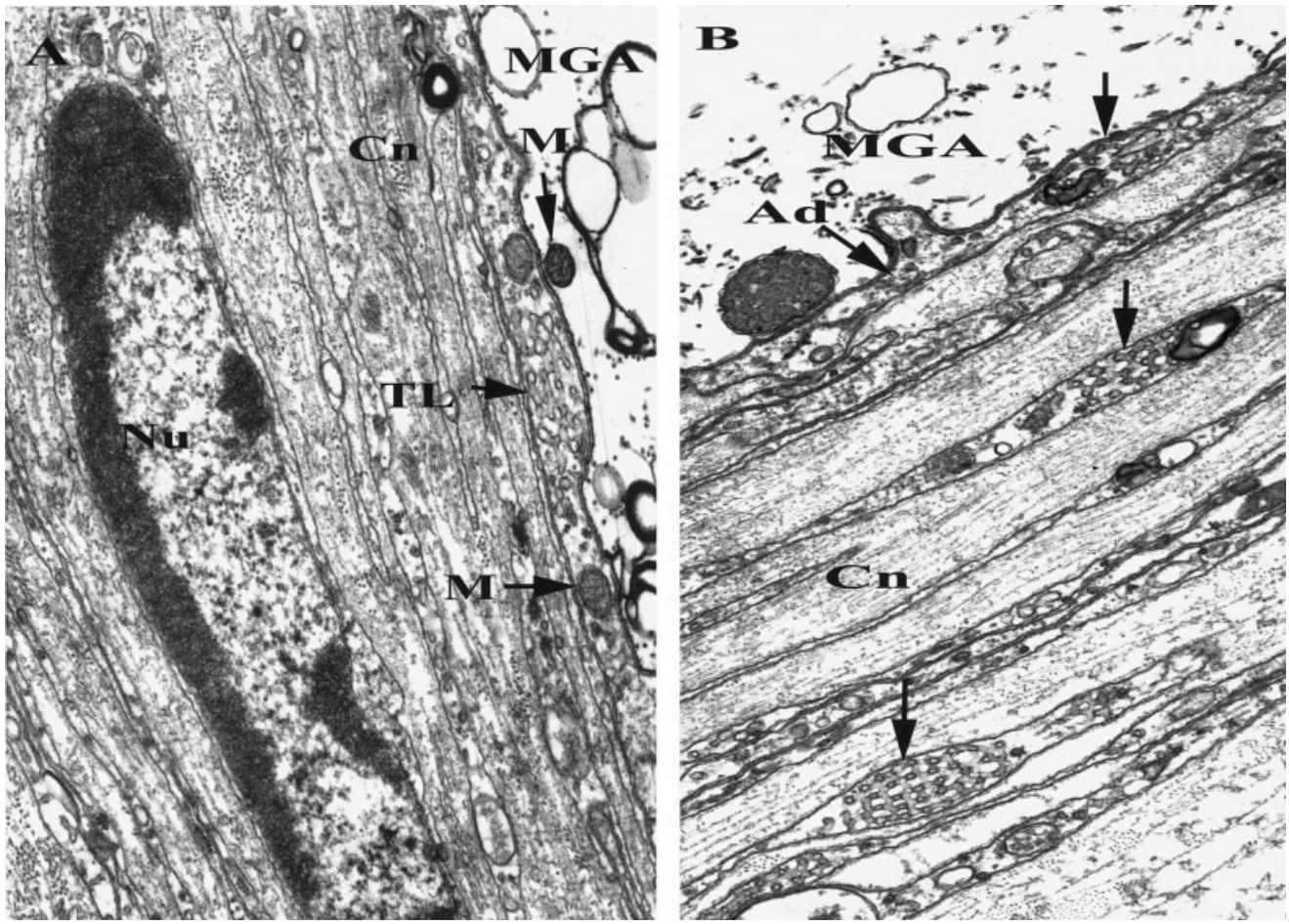

Fig. 5. Effect of 50-Hz/2-min stimulation on the morphology of the glial tubular lattice. **A:** Tubular lattice (TL) becomes swollen and losses its typical high degree of organization following high-frequency stimulation. Mitochondria (M) in both the adaxonal glial layer and the giant axon (MGA) and plasma membranes adjacent to the swollen tubular lattice appear normal. Similarly, the nucleus (Nu) of a glial cell in the periaxonal glial layer appears unaffected by stimulation. **B:** Electron micrograph illustrating that there is a gradient of stimulation-induced morphological change in the glial tubular lattice related to distance from the axon. The tubular lattice in the adaxonal glial cell (Ad) adjacent to the giant axon, identified by the arrow, is highly disorganized and the lumina of the tubular lattice expanded. A tubular lattice in the second layer of collagen (Cn) in the periaxonal glial layer, also marked by an arrow, exhibits less volume expansion, although still somewhat disorganized. The tubular lattice near the bottom of the panel, marked by the arrow, is typical of tubular lattice clusters not exposed to a stimulated axon. The tubular lattice is highly organized in a "string-of-beads" formation, interconnected with uniform diameter tubules.

tion or exogenous K^+. These results are to be expected if active transport and glial metabotropic receptors are important in K^+ clearance (Brunder and Lieberman, 1988; Hassan and Lieberman, 1988; Lieberman and Hassan, 1988). In contrast, metabolic poisons or metabotropic receptor agonists were reported to have no effect on K^+ clearance in the experiments reported by Inoue et al. (1997). Since the experiments by Inoue et al. (1977) were performed at 12°C on the giant fiber from the tropical squid, *Sepioteuthis*, acclimatized to water temperatures of ~30°C, it is possible that glial metabolic processes were slowed leaving them less responsive to metabolic poisons and receptor agonists or antagonists.

Nonetheless, diffusion must be considered a participating K^+ clearance mechanism operating in parallel with active mechanisms of clearance in crayfish medial giant nerve fibers. As shown by the results of the present study, tubular lattice structures lateral to the adaxonal space were less effected by stimulation the further from the axon they were found. This indicates that K^+ not taken up by the tubular lattice of the adaxonal glia diffused laterally to be taken up by tubular lattice further away. An earlier investigation (Pichon et al., 1987) reported that high-frequency stimulation of a crayfish nerve cord with an intact ion selective perineurial sheath caused a change in the sheath potential that was accounted for by K^+ accumulation at its internal face. The findings of this investigation and those of Pichon et al. (1987) are consistent with diffusion as a participant in K^+ clearance from stimulated nerve.

The critical experiments that implicate the tubular lattice as the K^+ uptake site were those related to the effect of the internal injection of the axon with TEA, a voltage-gated K^+ channel blocker (Shrager et al., 1969). The results demonstrated that volume expansion of the tubular lattice, resulting from high-frequency stimulation, was prevented by limiting the efflux of K^+ that normally accompanies action potential generation. There was little

likelihood that TEA, an impermeant ion, would have directly affected the glia since the agent was injected into the axon. Even in the event of TEA leakage from the down stream injection site, the tissue taken for analysis was up stream from that point and under constant superfusion in TEA-free medium preventing exposure of the glial investment to TEA.

There are at least two possible mechanisms for a K^+ uptake-induced volume expansion of the tubular lattice during action potential generation. The first is consistent with the findings of Wurtz and Ellisman (1986, 1989) that the volume expansion seen in the tubular lattice is a normal morphological event is that could be caused by the uptake of K^+ and obligated water which is preserved by gluteraldehyde fixation. A second possible explanation, also put forth by Wurtz and Ellisman (1986, 1989), is that the tubular lattice normally restricts free water movement through its membranes and takes up and compartmentalizes hyperosmotic concentrations of K^+. Tubular lattice volume expansion in the latter case occurs as a result of fixatives that cause the tubular lattice to lose their ability to restrict water movement. Although the presence or absence of aquaporins that could regulate water movements into the glial tubular lattice has not been investigated, it has been shown that the uptake of K^+ into crayfish glia occurs such that intracellular K^+ can increase to a concentration well above normal resting levels (Brunder and Lieberman, 1988).

The experiments described here do not differentiate between these two possible mechanisms. Nonetheless, either mechanism implicates a role for glial tubular lattice in K^+ uptake and its clearance from the adaxonal space during action potential generation in the nerve. The tubular lattice can accumulate ionic substances during the generation of propagated action potentials at high frequency, as seen with the accumulation of La^{3+} in vesicles produced by the swelling and apparent disaggregation of the tubular lattice. We propose that these vesicles represent the structure that sequesters and compartmentalizes K^+ released by the axon. The results of these experiments also suggest that stimulation-induced swelling of the tubular lattice and the nonuniform appearance of La^{3+} precipitate raise the possibility that some portion of the tubular lattice may not always be open to the extracellular space, a requirement for compartmentalization of K^+ taken up.

The experiments reported here provide evidence that the stimulation-induced swelling of the tubular lattice is reversible and causes no long-term damage to the electrical properties of the nerve. The tubular lattice of nerve fibers allowed a 10-min rest period following a period of high-frequency stimulation could not be distinguished from the tubular lattice of unstimulated nerve fibers.

In summary, taking advantage of an activity-dependent morphological change in the glial tubular lattice of the crayfish, we believe we have obtained the first experimental evidence for an active role for the tubular lattice of crayfish glia in adaxonal space K^+ homeostasis.

It would not be unreasonable to ask if the findings described here are limited to this particular invertebrate model and thus not more widely applicable. In this regard, there are significant parallels between the results reported here and in earlier investigations from this laboratory (Hassan and Lieberman, 1988; Lieberman and Hassan, 1988) on the effects of activity and extracellular K^+ homeostasis in the crayfish medial giant nerve fiber and that seen in nodes of Ranvier of frog peripheral nerve (Wurtz and Ellisman, 1986, 1988) and in astrocytes of the rat optic nerve (Ransom et al., 2000; MacVicar et al., 2002).

In the first case, Schwann cell folds overlying the node of Ranvier are highly interdigitated forming structures analogous to the tubular lattice of crayfish glia. These structures undergo volume expansion during repetitive stimulation. Wurtz and Ellisman (1986) also reported that when the node is fixed for electron microscopy immediately following stimulation, the formation of vacuoles within the nodal Schwann cell folds and separation from the axolemma is also seen. As in the present investigation, the microanatomical changes described in this report and by Wurtz and Ellisman (1986) were not seen following a short period of rest following the stimulation. They proposed that the activity-induced swelling and vacuolization following fixation was a consequence of the hyperosmotic accumulation of K^+ by the Schwann cell.

In the second case, Ransom et al. (2000) observed that rapid K^+ clearance from stimulated optic nerve was dependent on glial K^+ uptake via the Na pump while a second sustained slower component was dependent on axonal uptake. In an investigation that extended these findings, MacVicar et al. (2002) observed a reversible activity-induced volume change that could be mimicked by small increases in extracellular K^+ in an isolated optic nerve model. Activity-induced optic nerve volume changes could be reversibly inhibited by lowering extracellular K^+ or treating with TTX. Both activity- and high K^+-induced volume increases could be depressed by inhibition of the glial associated Na-K-2Cl cotransporter.

Taken as a whole, there is high degree of correspondence between K^+ homeostatic mechanisms used by the rat optic nerve, the frog peripheral nerve node of Ranvier, and the crayfish medial giant nerve fiber observed in the present and earlier investigations from this laboratory. These similarities suggest that the metabolic and structural mechanisms associated with activity-induced changes in glial volume, tubular lattice morphology and extracellular K^+ clearance observed in crayfish are upwardly conserved into mammalian species, thus providing an added level of confidence in the crayfish medial giant nerve fiber as a model for elucidating general principles of the role of glia in preservation of neural signaling.

ACKNOWLEDGMENT

This research was supported, in part, by a Sigma Xi grant-in-aid to P.H., a Neuroscience Student Summer Research and Education grant from the East Carolina

University Program in Neuroscience to J.E.B. and V.E.B., an Army Research Office (DOD) grant DAAG29-89-D0182 and NIH NS34799 to E.M.L. We also would like to thank Mr. Tim Charles, Department of Biology at East Carolina University for always being available to the authors for help and advice on electron microscopy methodologies used here.

REFERENCES

Abbott NJ, Lieberman EM, Pichon Y, Larmet Y. 1988. Periaxonal K^+ regulation in the small squid *Alloteuthis*: studies on isolated and in situ axons. Biophys J 53:275–279.

Adelman WJ Jr, Moses J, Rice RV. 1977. An anatomical basis for resistance and capacitance in series with the excitable membrane of the squid giant axon. J Neurocytol 6:621–646.

Brown ER, Abbott NJ. 1993. Ultrastructure and permeability of the Schwann cell layer surrounding the giant axon of the squid. J Neurocytol 22:283–298.

Brunder DG, Lieberman EM. 1988. Studies of axon–glia interactions and periaxonal K^+ homeostasis. I. The influence of K^+, Cl^- and cholinergic agents on the membrane potential of the adaxonal glia of the crayfish medial giant axons. Neuroscience 53:951–959.

Frankenhauser B, Hodgkin AL. 1956. The after-effects of impulses in the giant nerve fibres of *Loligo*. J Physiol (Lond) 131:341–376.

Hama K. 1961. Some observations on the fine structure of the giant fibers of the crayfishes (*Cambarus virilus* and *Cambarus clarkii*) with special reference to the submicroscopic organization of the synapses. Anat Rec 141:275–293.

Hargittai PT, Lieberman EM. 1991. Axon–glia interactions in the crayfish: glial cell oxygen consumption is tightly coupled to axon metabolism. Glia 4:417–423.

Hassan S, Lieberman EM. 1988. Studies on axon–glia interactions and periaxonal K^+ homeostasis. II. The effect of axonal stimulation, cholinergic agents and transport inhibition on the resistance in series with the axon membrane. Neuroscience 53:961–969.

Holtzman E, Freeman AR, Kashner LA. 1970. A cytochemical and electron microscope study of channels in the Schwann cells surrounding lobster giant axons. J Cell Biol 44:438–445.

Inoue I, Tsutsui I, Brown ER. 1997. K^+ accumulation and K^+ conductance inactivation during action potential trains in giant axons of the squid *Sepioteuthis*. J Physiol 500:355–366.

Lane NJ, Swales LS, Abbott NJ. 1977. Lanthanum penetration in crayfish nervous system: observations on intact and "desheathed" preparations. J Cell Sci 23:315–324.

Lieberman EM, Hassan S. 1988. Studies on axon–glia interactions and periaxonal K^+ homeostasis. III. The effect of anisosmotic media and potassium on the relationship between the resistance in series with the axon membrane and glial cell volume. Neuroscience 53:971–981.

Lieberman EM, Sanzenbacher E. 1992. Mechanisms of glutamate activation of axon-to-Schwann cell signaling in the squid. Neuroscience 47:931–939.

Lieberman EM, Villegas J, Villegas GM. 1981. The nature of the membrane potential of glial cells associated with the medial giant axon of the crayfish. Neuroscience 6:261–271.

Lieberman EM, Hargittai PT, Grossfeld RM. 1994. Electrophysiological and metabolic interactions between axons and glia in crayfish and squid. Prog Neurobiol 44:333–376.

MacVicar BA, Feigan D, Brown A, Rasom B. 2002. Intrinsic optical signals in the rat optic nerve: role for K^+ uptake via NKCC1 and swelling of astrocytes. Glia 37:114–123.

Orkand RK, Nicholls JG, Kuffler SW. 1966. Effect of nerve impulses on the membrane potential of glial cells in the central nervous system of Amphibia. J Neurophysiol 29:788–806.

Paracchia C, Robertson JD. 1971. Increase in osmophilia of axonal membranes of crayfish as a result of electrical stimulation, asphyxia, or treatment with reducing agents. J Cell Biol 51:223–239.

Pichon Y, Abbott NJ, Lieberman EM, Larmet Y. 1987. Potassium homeostasis in the nervous system of cephalopods and crustaceans. J Physiol (Paris) 82:346–356.

Ransom CB, Ransom BR, Sontheimer H. 2000. Activity-dependent extracellular K^+ accumulation in rat optic nerve: the role of glial and axonal Na^+ pumps. J Physiol (Lond) 522:427–442.

Shivers RR, Brightman MW. 1976. Transglial channels in ventral nerve cord of crayfish. J Comp Neurol 167:1–26.

Shrager PG, Macey RI, Strickholm A. 1969. Internal perfusion of crayfish giant axons: action of tannic acid, DDT, and TEA. J Cell Physiol 74:77–90.

Shrager PG, Starkus JC, Lo M-VC, Peracchia C. 1983. The periaxonal space of crayfish giant axons. J Gen Physiol 82:221–244.

Wallin BG. 1967. The relation between external potassium concentration, membrane potential and internal ion concentrations in crayfish axons. Acta Physiol Scand 70:431–448.

Weibel ER. 1979. Stereological methods. Vol. 1: Practical methods for biological morphometry. London: Academic Press.

Wurtz CC, Ellisman MH. 1986. Alterations in the ultrastructure of peripheral nodes of Ranvier associated with repetitive action potential propagation. J Neurosci 6:3133–3143.

Wurtz CC, Ellisman MH. 1988. Activity associated ultrastructural changes in peripheral nodes of Ranvier are independent of fixation. Exp Neurol 101:87–106.

Zwahlen MJ, Sandri C, Greeff NJ. 1988. Transglial pathway of diffusion in the Schwann sheath of the squid giant axon. J Neurocytol 17:145–159.